Polar Science 23 (2020) 100502

Contents lists available at ScienceDirect

Polar Science

journal homepage: http://www.elsevier.com/locate/polar

Hot-water coring system with positive displacement motor

An Liu, Yang Yang *, Xiaopeng Fan, Liang Wang, Dayou Fan, Xingchen Li, Pavel G. Talalay

Polar Research Center, Jilin University, No. 938 Ximinzhu Str., Changchun City, 130021, China

A R T I C L E I N F O

Keywords:
Ice drilling
Hot-water ice-coring
Positive displacement motor

A B S T R A C T

In this study, a new coring system is designed that uses a positive displacement motor (PDM) connected to a core barrel and drill bit in combination with a hot-water drilling (HWD) system. The surface equipment and water hose are shared and the hot-water drill nozzle is replaced by the corer when a borehole is made by HWD. The hot water is then utilized to drive the PDM corer. In this paper, the concept of the PDM coring system is presented, along with a novel self-adaptable anti-torque device that can automatically adjust the diameter to adapt to an irregular borehole. The required force-energy parameters of the PDM are theoretically estimated. A PDM coring system is designed and assembled, and the feasibility of the concept is tested in the laboratory. The results indicate that it is more conducive to perform the coring at a lower temperature of water. At a temperature of 5 °C, a double-walled core-barrel works adequately to produce ice cores with a maximum diameter of 73 mm and an inner barrel diameter of 79 mm at a water flow rate of 96 L/min.

1. Introduction

Hot-water drilling (HWD) is regarded as the fastest drilling method in the polar regions, where it is mainly used to gain access to the base of an ice sheet or ice shelf for varying types of research (Engelhardt et al., 1990; Bentley and Koci, 2007; Makinson et al., 2016).It was used to obtain direct oceanographic observations of the basal melt rate of Antarctic ice shelves (Makinson, 1994; Rignot et al., 2013; Makinson and Anker, 2014; Sugiyama et al., 2014) and search for neutrinos using clear glacial ice as the detecting medium (Lowder et al., 1991; Silvestri, 2005). HWD technology has been extensively used in glaciological investigations with excellent results and high reliability, except for its limitation when used for non-core drilling. In fact, subglacial cores are of importance since these cores provide opportunities for understanding the interplay of dynamic processes of the Earth (Talalay and Pyne, 2017) and reconstructing biological evolution and paleoclimatic and global environmental changes (Langway, 2008). New coring devices must be devised in combination with a HWD system for obtaining core samples from particular depths that might be of scientific interest or for drilling through formations such as rocks and ice tills. In this regard, a hot-water ice-coring drill was designed by Engelhardt from Caltech, which was an annulus core barrel with coring head equipped multiple jets. Several attempts were made in the 1990s to recover ice from the base of the West Antarctic ice streams using this coring method (Engelhardt et al., 2000). Since then, this type of ice-coring drill has often been used in the polar regions to retrieve ice cores from selected depths (Jackson and Kamb, 1997; Makinson, 2006). However, the hot water used for melting the ice simultaneously melts the ice core; therefore, the cores obtained by the coring drill are frequently fragmentary (Craven et al., 2009). At times, a core cannot be retrieved as its diameter is extremely small and it cannot be caught by the core dogs (Nicholls et al., 2012; Vogel et al., 2005).

In an attempt to overcome these limitations of hot-water coring drilling, mechanical drilling coupled with a HWD system was suggested, as a mechanical drill is typically able to acquire ice cores that are regular and relatively intact (Bentley et al., 2009; Casey et al., 2014). Koci (1994) proposed a type of ice coring method that used a positive displacement motor (PDM) with a core barrel and drill bit. Tests of the prototype coring drill were performed in an ice drill test well constructed by the University of Alaska; however, details of the testing results were not provided (Das et al., 1992). Further research on the PDM corer must be specifically carried out to recover cores faster and of better quality.

A PDM is a type of downhole tool whose main feature is the ability to convert the hydraulic pressure energy of a liquid into rotation (Nguyen et al., 2018). It basically consists of four parts: a bypass-valve, motor, versatile spindle, and transmission shaft (Baldenko and Korotaev, 2002). The motor includes a housing (stator) and shaft enclosed in the stator (rotor). The shaft has a wave-shaped cross-section and each wave corresponds to a lobe (Fig. 1).

The drilling fluid describes a helical path between the shaft and

* Corresponding author.
E-mail address: yangyang2014@jlu.edu.cn (Y. Yang).

https://doi.org/10.1016/j.polar.2019.100502
Received 21 June 2019; Received in revised form 11 December 2019; Accepted 24 December 2019
Available online 27 December 2019
1873-9652/

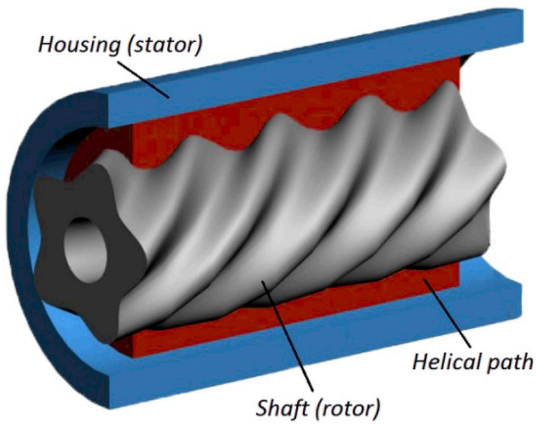

Fig. 1. Sectional view of motor.

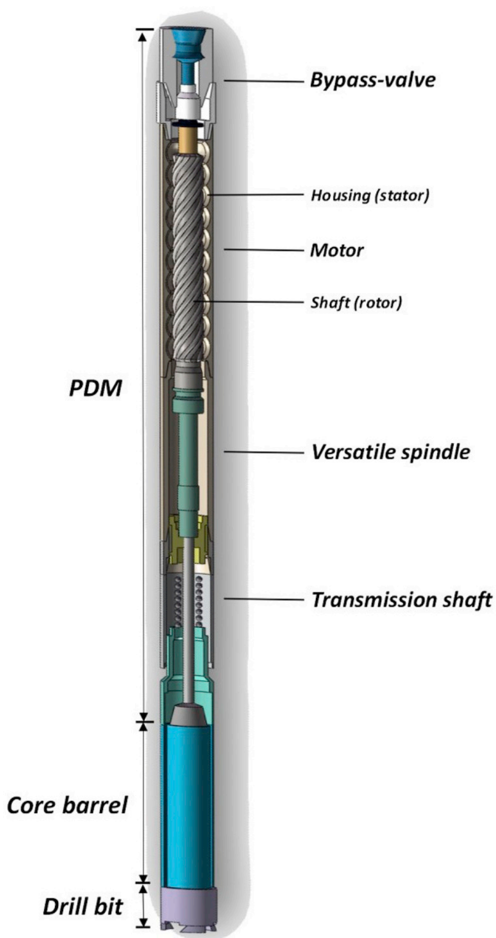

Fig. 2. Schematic of PDM corer.

housing forcing the shaft to rotate clockwise. The eccentric rotation of the shaft is converted to a concentric rotation by the versatile spindle that is connected to the transmission shaft. The prominent advantages of a PDM are described:

- The hot water PDM can drive a rock drilling bit.
- It has a rugged design and is suitable for different types of regions, including the polar regions.
- A fluid can be used as power. Conventional drilling fluids, such as aqueous ethylene glycol and ethanol solutions, as well as innovative drilling fluids, like water and air at high pressure, can be used to drive the PDM.
- The output torque and rotational speed are directly proportional to the pump pressure and flow rate, respectively. Therefore, drilling parameters, such as the torque and rotational speed, can be adjusted individually according to the requirements of the drilling.

In view of such features, a PDM is the appropriate power device for use in combination with a HWD system and was utilized in rapid access drilling and ice extraction (RADIX drill) by the University of Bern in Switzerland, using ESTISOL 140 or silicone fluid as the hydraulic power (Schwander et al., 2014). In this study, a PDM coring system was designed to meet the coring needs of HWD at a certain depth. The required force-energy parameters were theoretically estimated and laboratory tests were performed to demonstrate its feasibility and effectiveness.

2. General concept of PDM coring system

The hot-water drill nozzle is replaced by the PDM coring system when a borehole is made by HWD. High-pressure water of a HWD system is utilized to power the PDM, with the hot water acting as chip transport as well as a melting medium. Fig. 2 displays the schematic of a PDM corer.

The field operation protocol is as follows (Fig. 3):

(a) First, the HWD system that includes a winch and high-pressure pump, and a boiler are installed in the desired area. The hot-water drill starts to drill the ice.
(b) At the desired depth, the PDM corer replaces the hot-water drill and is prepared to be lowered.
(c) The PDM corer is lowered and water at a high pressure starts to drive the PDM operation. The PDM corer commences the drilling and coring.
(d) Finally, the PDM corer is lifted to the surface after the coring and the cores are released.

2.1. Chinese HWD project

The Chinese HWD project was initiated in 2011 by the Polar Research Institute of China in alliance with other universities. The aim of this project was to build an HWD system to drill rapidly through an ice shelf of thickness 1500 m. Further objectives were to place a number of oceanic observation devices into the borehole, establish a monitoring platform for ice sheet–ice shelf–ocean interplay, and investigate the freezing or melting processes beneath the ice shelf and mass balance of the ice sheet. In 2017, laboratory tests of this system were successfully performed in the Key Lab of the Ministry of Natural Resources, located in the Jilin University. This was a significant step in the production of Chinese HWD systems with the ability to drill through an ice shelf, thousands of meters in thickness, within a few days. Table 1 shows the detailed specifications of the Chinese HWD system.

The environment of ice below an ice shelf is quite intricate. Warmer water from the deep ocean melts the base of the ice shelf, the melted water moves up along the slope under the ice shelf and refreezes in various forms, e.g., slush ice, permeable marine ice, and solid marine ice (Fig. 4). Generally, a direct observation cannot provide a comprehensive analysis (such as ice fabric research) and the best method of studying bottom ice is still to obtain ice cores; therefore, it is important to design a suitable hot-water coring system.

2.2. Design of key devices based on Chinese HWD

The anti-torque system is initially installed on the top end of the PDM corer to prevent the upper non-rotating part of the corer from spinning.

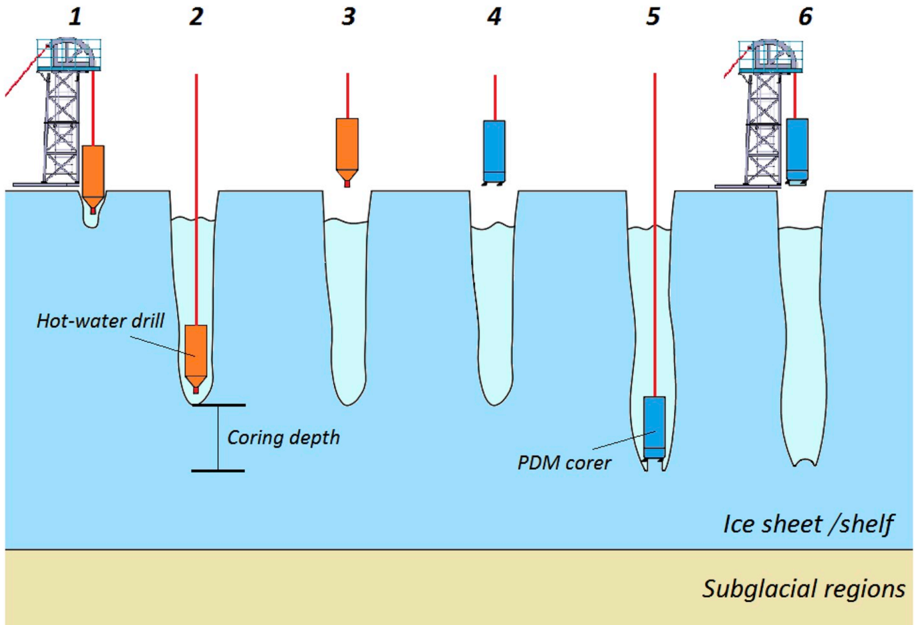

Fig. 3. PDM corer access operation.

Table 1
Specifications of the Chinese HWD system.

Flow rate	Pump pressure	Length of hose	ID of hose	Hose turns on winch drum	Winch speed	ROP (Rate of penetration)	Borehole Diameter
220 L/min	9 MPa	2200 m	38 mm	440	0–0.5 m/s	38 m/h	35–60 cm

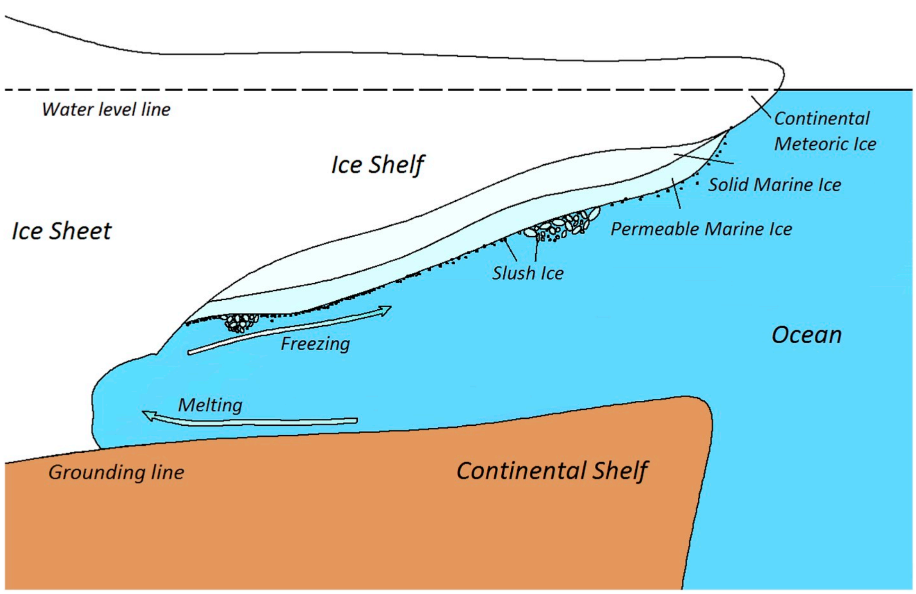

Fig. 4. Melting and freezing of ice below an ice shelf.

The diameter of the anti-torque part must be nearly the same as the inner diameter of the borehole. Unlike in mechanical drilling, the boreholes created by HWD are large and irregular therefore, some modifications must be made to the normal anti-torque part to adapt it for this system. Many types of anti-torque systems were used in ice drilling such as hinged friction blades, leaf springs, skates, side milling cutters, and U-shaped blades (Fan et al., 2016). Among these, the leaf spring and skate anti-torque systems are proven to be the most reliable designs. The main difference between them is the torque that they can withstand. Generally, a skate anti-torque system provides a higher anti-torque than a leaf spring; however, a remarkably high torque is not required while drilling in ice. Thus, a leaf spring anti-torque system may be considered, owing to the following advantages: (1) it is mechanically simple, (2) the springs are elastic to allow easy passage over any irregularities in the borehole. In view of the above features, the leaf spring anti-torque system is used in the PDM coring system to fit the HWD adequately. The diameter of the spring must be adjusted to be sufficiently large and nearly the same as the diameter of the borehole made by the HWD.

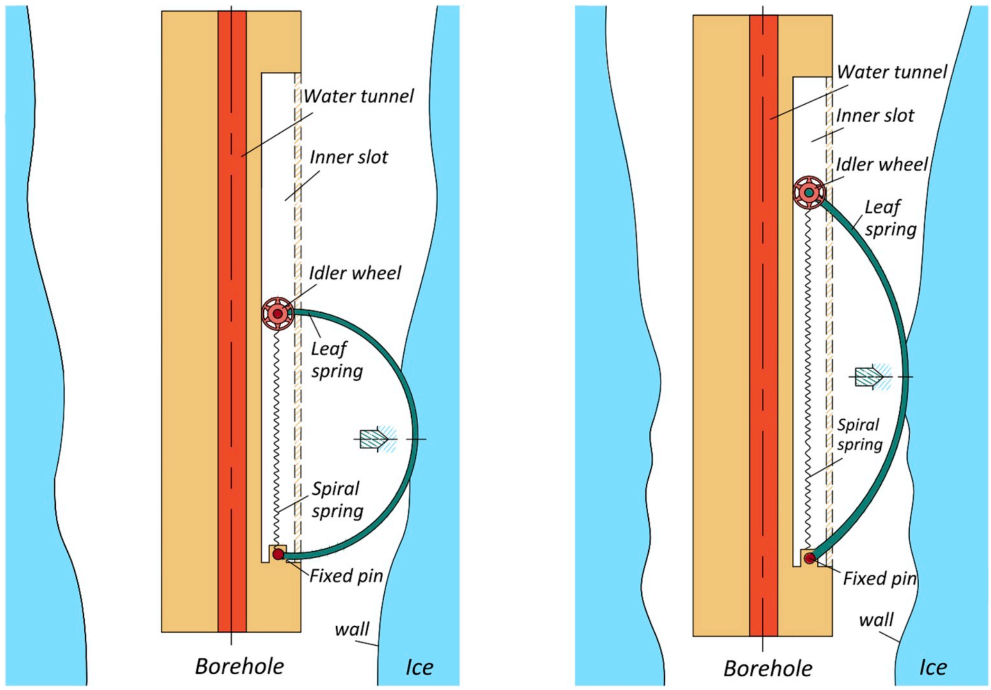

Fig. 5. Working schematic of the self-adaptable leaf spring anti-torque device: the left side shows the position with the leaf spring significantly deformed against the wall of a borehole with a large diameter; the right side shows the position with the spiral spring fully extended to adapt to a borehole with a small diameter.

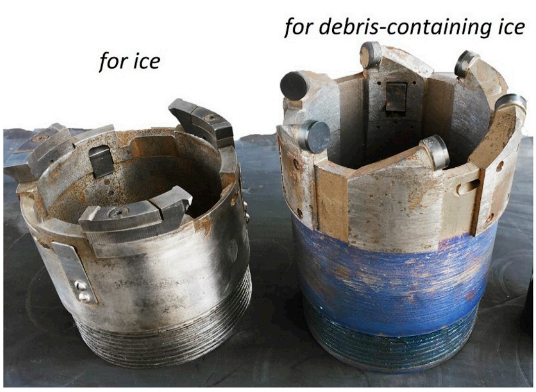

Fig. 6. Two types of drill bits used in ice drilling.

Further, the diameter of the spring must be adjustable to adapt to boreholes with irregular shape and diameter as the diameter of a borehole ranges between 35 and 60 cm.

A new self-adaptable anti-torque device is designed to meet these requirements and its working principle is shown in Fig. 5. The top end of the leaf spring is connected to idler wheels that are installed in an inner slot and constrained in the radial direction by its outer wall but can move freely along the axial direction. The bottom end of the leaf spring is fixed to the lower part of the inner slot by a fixed pin. A spiral spring of high elasticity is retracted and installed between the top and bottom ends of the leaf spring. This is done to hold the idler wheels to make the leaf springs elastically deformed and press on the borehole wall against rotation. The leaf spring can be inserted into ice deeply and provides a reliable anti-torque, owing to its sharp fringe. When the diameter of a borehole changes dramatically, for example, decreasing from a large to small value during tripping, the leaf spring is subjected to an inward radial force applied by the wall. When this force increases sufficiently to become larger than the force that the spiral spring applies on the idler wheel, the spiral spring is elongated; hence, the idler wheel accompanied by the top end of the leaf spring moves up immediately. The

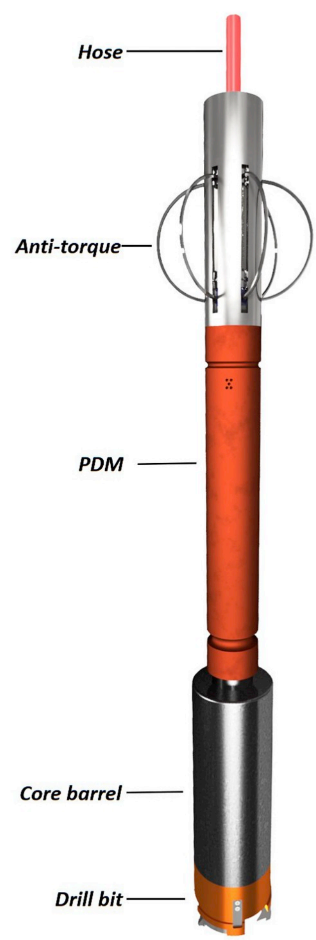

Fig. 7. PDM coring system.

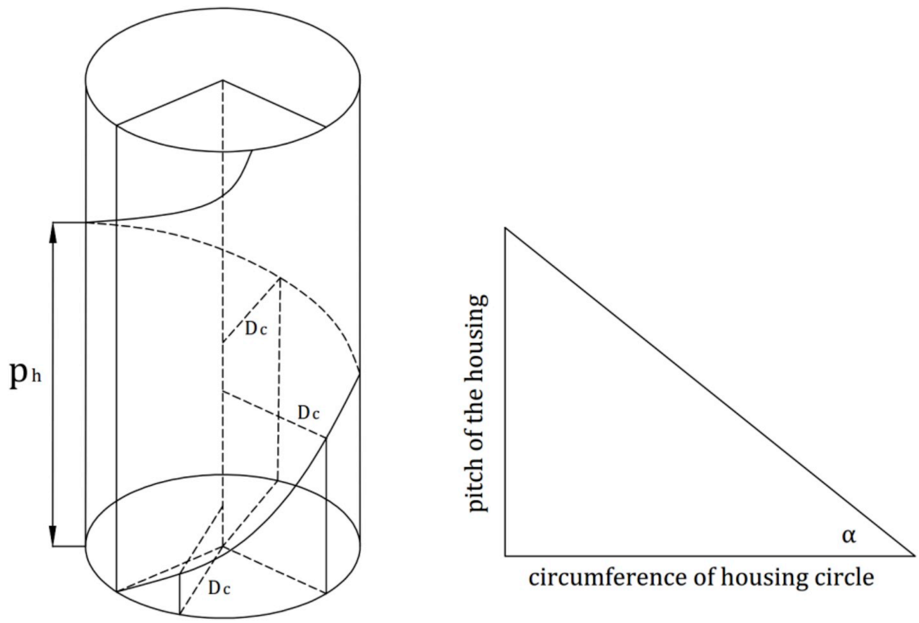

Fig. 8. Helix angle.

Table 2
Unit conversion.

Parameter	Unit	
M_T	1 Nm	0.723 ft·lb
Δp	1 MPa	145 psi
q	1 L	61 cu.in

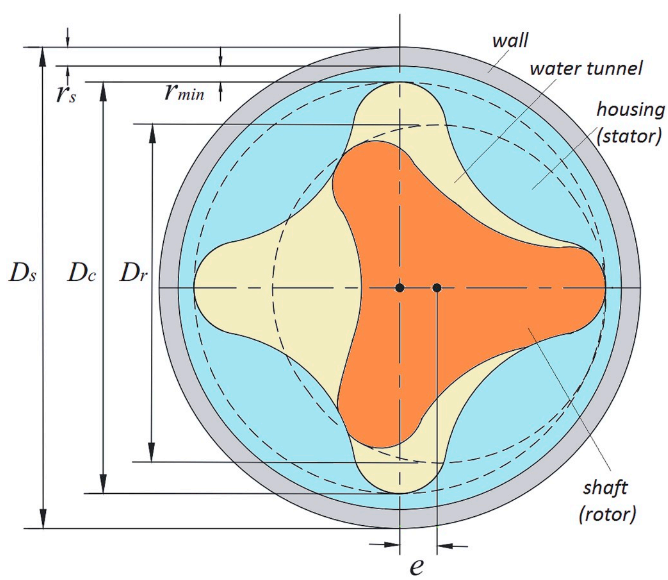

Fig. 9. Cross-sectional view of a motor with a 3:4 lobe Robles (2001).

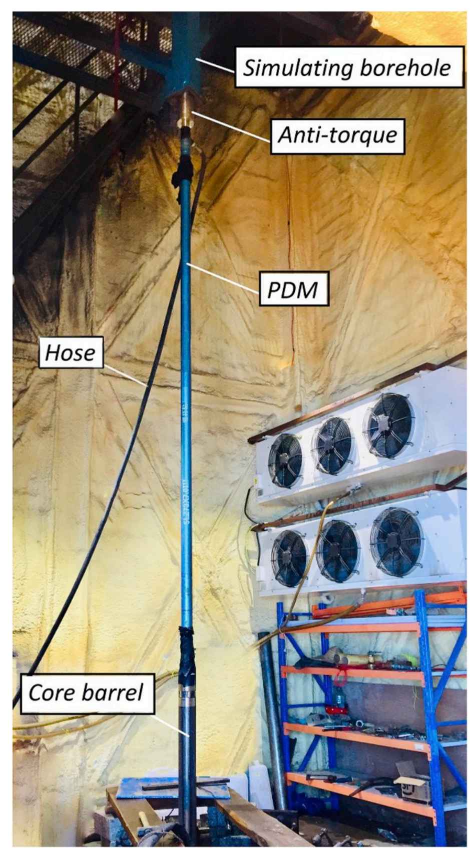

Fig. 10. PDM coring system in the laboratory.

Table 3
Technical parameters of the designed PDM.

Bit Size	Outer Diameter	Pressure Drop	Flow Rate	Rotation Speed	Torque
136 mm	86 mm	0.33 MPa	0–220 L/min	0–200 rpm	30 Nm
Displacement Per Revolution		**Lobe Number**	**Diameter of Rotor**	**Diameter of Stator**	**Motor Eccentricity**
0.66 L/r		3:4	38 mm	56 mm	9 mm

diameter of the leaf spring then decreases until a new force balance state is achieved between the spiral spring, leaf spring, and borehole wall to adapt to the variation in the shape of the borehole. The opposite situation occurs if the diameter of a borehole increases. Six such mechanisms are distributed around the device and work independently to a full extent, meeting an irregular borehole wall in most of the directions. Moreover, hot water can still pass through the water tunnel in the center of the device while drilling.

Different types of drill bits were designed to retrieve cores from various ice layers (Fig. 6). Cutters of the drill bit on the left side were made with high-speed steels that were designed for pure ice. The drill bit on the right side was designed for debris-containing ice; hence, the cutters were made with polycrystalline diamond compact.

A complete schematic of the coring system is shown in Fig. 7. The water hose and PDM were connected to the top and bottom ends of the anti-torque device, respectively. The core barrel with the drill bit was at the lower end of the PDM and all the parts were connected by a screw thread.

2.3. Theoretical estimation of required PDM parameters

As a critical part of the coring system, the main force-energy parameters of the PDM such as the total pressure drop, output torque, and displacement per revolution must be predetermined. These parameters that affect the working performance of the PDM as well as that of the entire coring system are calculated according to the specifications of the Chinese HWD system to improve the relevance and efficiency.

2.3.1. Pressure drop

First, the pressure loss during the transportation of water in the hose from the winch to drill and the water pressure remaining when water moves to the PDM were calculated. The pressure loss includes two parts: frictional pressure loss ΔP_1 and local pressure loss ΔP_2, so that the total pressure loss, ΔP, is

$$\Delta P = \mu(\Delta P_1 + \Delta P_2) \tag{1}$$

where, μ is the dimensionless safety factor assumed to be 1.5.

$$\Delta P_1 = \lambda \frac{l}{d} \times \frac{\rho v^2}{2} \tag{2}$$

Table 4
Main parameters of the test equipment and sensors.

Equipment and sensors	Model	Main parameters
High-pressure pump	SHP 75-100	Power 18 kW Maximum pressure 5 MPa Maximum flow rate 160 L/min Weight 1100 kg
Flow sensor	LWGB-DN25	16–160 L/min
Temperature sensor	HSTL-103	0–100 °C
Load sensor	MIK-LCLY	Maximum weight 200 kg
Encode	E6B2-CWZ6C	Resolution 600 P/R
Heater		Power 4 × 10 kW
Submersible pump	QDX2	Pump head 15 m Flow rate 10 m^3/h Power 0.75 kW

where, ΔP_1 is the frictional pressure loss (MPa), l is the length of the hose (2200 m), d is the inner diameter of the hose (0.038 m), v is the velocity of water in the hose (m/s), ρ is the density of water (1000 kg/m^3), λ is the frictional coefficient, which is dimensionless and related to the Reynolds number (Re) as given below:

$$\mathrm{Re} = \frac{\rho v d}{\upsilon} \tag{3}$$

where, υ is the dynamic viscosity of water. It varies slightly when the temperature of water changes but has little effect on the result and therefore, is regarded as a constant in the calculations. The temperature of the hot water used in the coring system is approximately 50 °C. At this temperature, its dynamic viscosity is 5.494×10^{-7} m^2/s (Haynes, 2017).

In addition,

$$v = \frac{Q}{A} \tag{4}$$

where, Q is the flow rate (220 L/min) and A is the cross-sectional area of the hose (m^2). According to Eqs. (3) and (4), the Reynolds number is determined to be 223619, which is in the range of 1×10^5–3×10^6. Thus, the water in the hose is in a state of turbulence and the frictional coefficient is calculated by the following equation (White, 2011):

$$\lambda = 0.0032 + \frac{0.221}{\mathrm{Re}^{0.237}} = 1.51 \times 10^{-2} \tag{5}$$

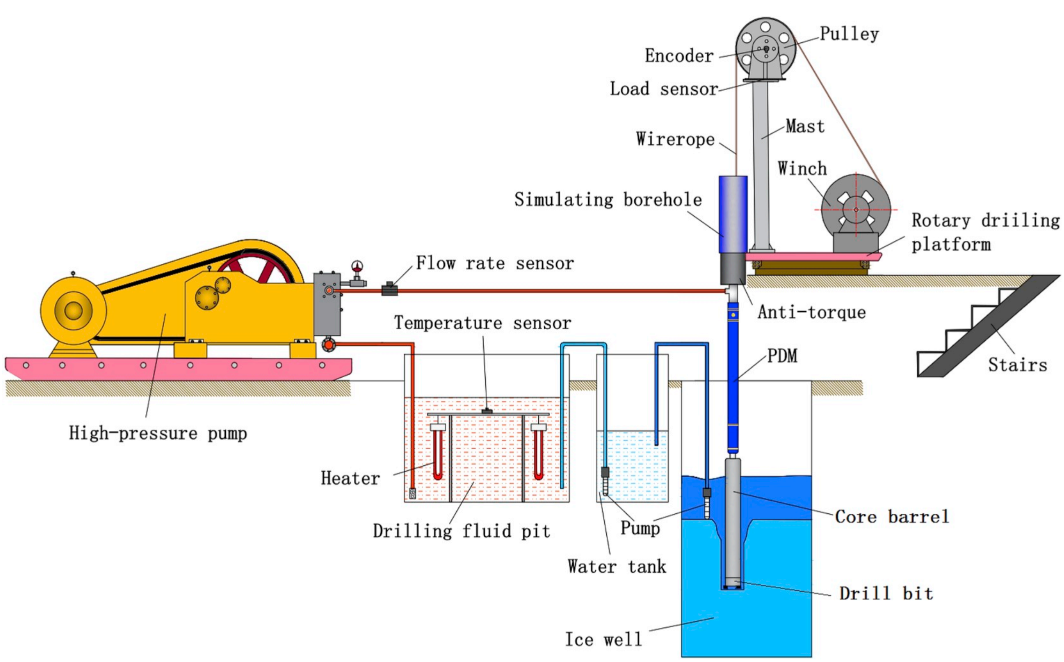

Fig. 11. Schematic of the testing PDM coring system.

Table 5
Main results of the PDM coring system tests.

No.	Barrel type*	ID/OD of bit (mm)	Water temperature (°C)	Flow rate (L/min)	Depth (mm)	Core diameter (mm)	Radial coring rate*	Core length (mm)	Axial coring rate*	Diameter of borehole (mm)	ROP (m/h)
1	SW	105/136	50	96	500	52	0.50	112	0.22	317	10.4
2	SW	105/136	25	96	500	73	0.70	251	0.50	242	9.1
3	SW	105/136	5	96	500	96	0.91	418	0.84	195	7.9
4	DW	79/110	5	96	500	73	0.93	427	0.85	147	5.7

*SW – single-walled core barrel; DW – double-walled core barrel.
*Radial coring rate – Ratio of the core diameter to inner diameter of the core barrel.
*Axial coring rate – Ratio of actual core length to borehole depth.

Fig. 12. Overview of the PDM coring system tests:
(a) drill in the ice well; (b) drill bit with the ice core; and (c, d) ice core measurements.

All the values are substituted in Eq. (1), and ΔP_1 is evaluated to be 4.58 MPa.

In addition,

$$\Delta P_2 = \xi \frac{\rho v^2}{2}, \tag{6}$$

where, ξ is the local pressure loss coefficient that is calculated by the following equation (White, 2011):

$$\xi = \left(0.131 + 1.847\left(\frac{r}{R}\right)3.5\right)\ \frac{\theta}{90^\circ}, \tag{7}$$

where, θ is the bending angle of the hose. As there are 440 turns on the winch, $\theta = 440 \times 360^\circ = 158400^\circ$, r is the radius of the hose (0.019 m), and R is the bending radius (1–2 m). The value of r/R is negligible, hence, the value of ξ is 230.6. Thus, ΔP_2 is determined to be 1.21 MPa.

The total pressure loss is calculated to be 8.67 MPa and the maximum pressure that the pump can supply is 9 MPa. Therefore, the pressure drop of the PDM should be designed to be not more than 0.33 MPa; otherwise, it will not operate.

2.3.2. Displacement per revolution

The displacement per revolution depends only on the structures of the rotor and stator that determine the rotation speed of the PDM and is calculated by the following equation:

$$q = \frac{Q}{a}\eta_v \tag{9}$$

where, q is the displacement per revolution (L/r), and η_v is the volume efficiency. It is dimensionless and $0.6 \le \eta_v \le 0.9$. The minimum efficiency is chosen to ensure sufficient working ability; thus, η_v is assumed to be 0.6. The rotation speed, a, of the PDM, generally depends on the type of the drill bit used at a given pressure on the PDM inlet and Q. Different revolutions per minute (rpm) are recommended for different formations, e.g., for ice drilling, the rpm must be approximately 50–230 (Talalay, 2003) whereas it is 100 as suggested by the theoretical estimation (Talalay et al., 2014). With a safety factor of 2.0, the assumed rpm must be 200. The displacement per revolution is calculated to be 0.66 L/r when all the values are substituted in Eq. (9).

2.3.3. Output torque

Generally, drilling in ice does not require a large torque and the normal range is typically between 10 and 20 Nm. The test results of the Polar Research Center of Jilin University suggested a torque of 15 Nm for ice drilling. The torque of the PDM should not be less than 15 Nm taking into consideration the additional torque generated by friction, thus, the output torque must be 30 Nm with a safety factor of 2.0.

2.3.4. Optimal lobe number

The lobe number is the ratio of the screw number of the rotor to that of the stator and largely determines the working ability of the PDM. A large value of the lobe number implies a high working ability and vice versa. Therefore, a suitable lobe number for HWD must be estimated as a large lobe number causes wastage of energy whereas a PDM with a smaller lobe number cannot operate with the system. The lobe number is calculated according to the equation given below (Samuel, 1997):

$$q = 2.46\left(\frac{1 - i^2}{(2 - i)^2}\right) D_c^3 \tan\alpha \tag{10}$$

$$M_T = 0.01\Delta pi\left(\frac{1 + i}{(2 - i)^2}\right) p_h D_c^2 \eta \tag{11}$$

$$i = \frac{n}{n + 1} \tag{12}$$

where, q is the displacement per revolution (L/r), ΔP is the total pressure loss (MPa); i is the winding ratio; n is the number of rotor lobes; M_T is the torque of the PDM; η is the gross efficiency, $0.4 \le \eta \le 0.7$ (the minimum efficiency should be considered; hence, $\eta = 0.4$); D_c is the maximum diameter of the housing (mm); α is the helix angle (Fig. 8); and p_h is the pitch of the housing, which can be expressed in terms of α by the following equation:

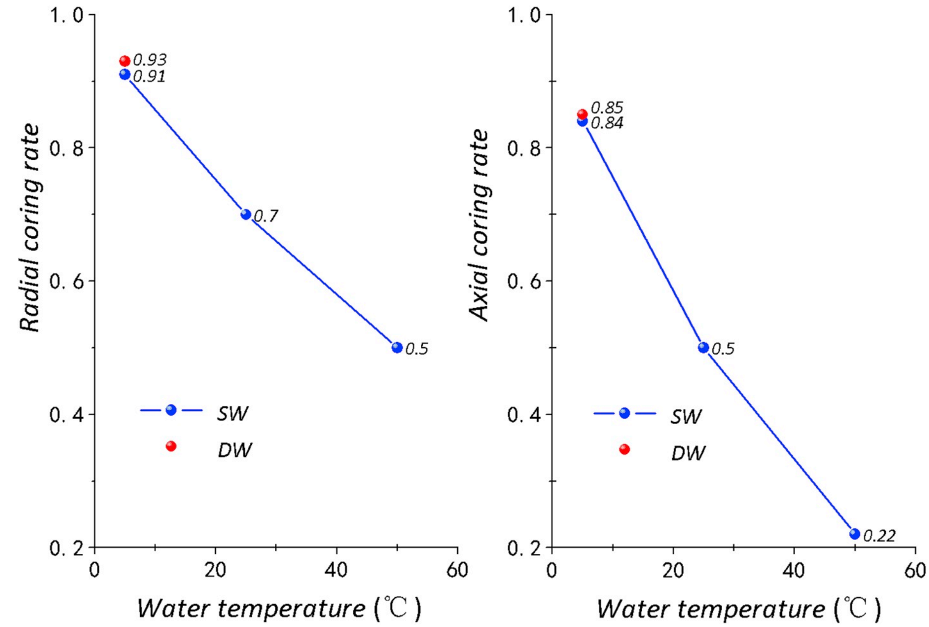

Fig. 13. Coring ratio at different water temperatures with two types of core barrels (SW - single-walled core barrel; DW - double-walled core barrel).

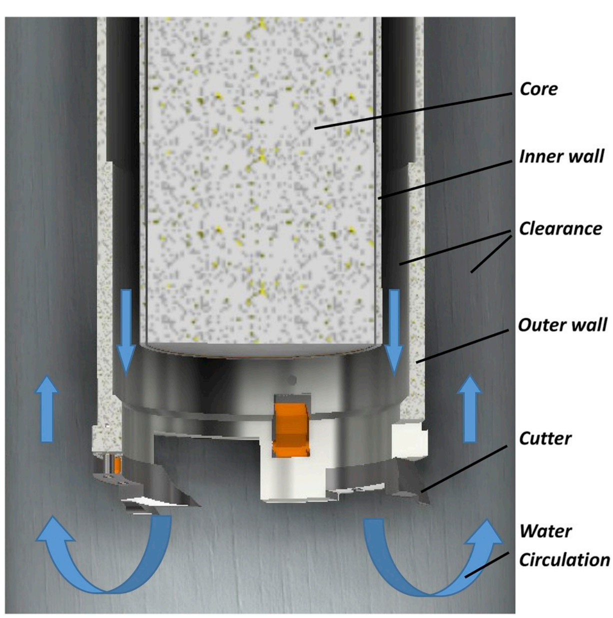

Fig. 14. Cross-section of double-walled core barrel.

$$\tan \alpha = \frac{p_h}{\pi D_c} \tag{13}$$

Eq. (14) is obtained by rearranging Eq. (10) – (13) as given below:

$$n = \frac{246 M_T}{\pi \Delta p q \eta} \tag{14}$$

In this equation, M_T, q, and Δp are in the units of ft·lb, cu.in, and psi, respectively, and must be converted to the units of Nm, L, and MPa, respectively, according to Table 2.

The value of n is approximately equal to 2.2 after all the values are substituted into Eq. (14). As n should be an integer not less than 2.2, its value is taken to be 3. The number of rotor and stator lobes is 3 and 4, respectively, and the value of i is calculated to be 0.75.

2.3.5. Diameters of rotor and stator

D_c is the maximum inner diameter of the housing (Fig. 9) and is obtained by the following equation (Su, 2001):

$$D_s = D_c + 2r_{\min} + 2r_s \tag{15}$$

D_s is the outer diameter of the PDM that depends on the diameter of the drill bit. Generally, the distance between the inner wall of the borehole and outer wall of the PDM should not be less than 25 mm to ensure an unhindered circulation of the drilling fluid. The diameter of the drill bit is 136 mm; therefore, D_s is calculated to be 86 mm. $r_{\min}$ is the thickness of the housing and different thicknesses are recommended, based on different drilling fluids. A value of $r_{\min}$ of 10 mm is assumed for high-temperature water (Han et al., 2014). r_s (5 mm) is the thickness of the wall and $D_c = 56$ mm.

Moreover,

$$\frac{D_r}{D_c} = \frac{n}{n+1} = i \tag{16}$$

where, D_r is the diameter of the shaft (rotor) and is equal to 38 mm according to Eq. (16), and

$$D_c - D_r = 2e \tag{17}$$

where, e is the eccentricity of the motor. This eccentricity is defined as the difference between the radii of the stator and rotor and is calculated to be 9 mm.

All the parameters of the designed PDM are listed in Table 3.

3. Test of feasibility

A prototype PDM coring system was designed to test the feasibility, as shown in Fig. 10. A square pipe was used to simulate the borehole. An anti-torque system with a diameter nearly equal to the inner diameter of the hollow pipe was inserted into the simulating borehole and acted on its inner wall to prevent rotation. The lower part was the PDM connected to the core barrel and drill bit.

The tests with the coring system were performed in an ice drilling test facility (Wang et al., 2018). The ice well in this facility had a Φ 1 m × 12.5 m at a minimum ice temperature of −30 °C. The ice temperature could be adjusted by a temperature sensor according to the actual requirement and was always set to −20 °C in these tests. The schematic of the test is shown in Fig. 11. The coring system was suspended over the ice well using the wire rope of the rotary drilling platform. The wire rope passed over the pulley and was connected to the winch, whose rotation speed was adjusted using a control box by changing the frequency to vary the lifting and lowering speeds of the coring system.

Water in the drilling pit was heated and then pumped through the hose by the high-pressure pump into the coring system. It was then sprayed out to melt the ice for penetration. When one drilling run was over, the water in the ice well was collected in the water tank by a submersible pump and pumped into the drilling pit and heated again for the next run. Several types of sensors were installed, including a flow meter at the outlet of the high-pressure pump, load sensor underneath the pulley, and temperature sensor in the drilling fluid pit, which was used to measure the temperature of the heated water. The load sensor was used to check whether the drill bit touched the ice, because there would be a change in the load if it went down extremely rapidly and touched the ice. Therefore, according to the feedback, the downward speed of the drill was adjusted by controlling the winch to maintain an optimal weight on the bit. The data of the penetration rate and drilling depth were obtained by the encoder installed on one side of the pulley. All the parameters of the equipment and sensors are listed in Table 4.

The testing procedure included four tests that were performed by three personnel in the laboratory at an air temperature of approximately −15 °C (Table 5, Fig. 12). Owing to the limitation created by the height of the laboratory, the core barrel was not designed to be long; hence, the depth of each run was only 500 mm. All the tested flow rates were nearly 96 L/min. First, a single-walled core barrel was used and tested at a water temperature of 50 °C. However, the core that was retrieved was of quite an inferior quality and subsequently, the water temperature was adjusted to 25 °C. However, the quality of ice core obtained was still inferior. During the 3rd run, an ice core of relatively good quality was obtained when the temperature of the water was 5 °C. At the same temperature, a double-walled barrel was tested instead of the single-walled core barrel and quality ice cores were retrieved.

The results showed that the high-temperature water used in the HWD system was not applicable to drive the PDM as it melted the ice core. This problem was solved by using water at a lower temperature to protect the ice core while still melting the ice chips. A temperature of 5 °C was suggested because at this temperature, the PDM coring drill obtained cores with a maximum axial ratio of 0.84 and radial ratio of 0.91 when a single-walled core barrel was used. In comparison, the maximum axial ratio was 0.85 and radial ratio was 0.93 when using a double-walled core barrel at a water flow rate of 96 L/min (Fig. 13), which showed that the working of the PDM coring system was adequate.

The results also showed that the quality of the cores obtained with the double-walled core barrel was better than that obtained with the single-walled core barrel, as the ice core could be stored in the inner wall of the double-walled barrel. Moreover, the water passed through the space between the walls and did not directly flush the ice core and prevented it from melting, which is very important in coring. Therefore, it is advisable to use the double-walled core barrel in future design.

According to the coring rate data, the diameter and length of the core barrel must be predetermined to ensure that the cores meet the requirements. For example, if the desired core diameter is 108 mm with a maximum radial coring rate of 0.92, the inner diameter of the core barrel must not be less than 118 mm.

Other optimization measures to be considered to obtain ice cores of improved quality are the following: (1) It is advisable to ensure that the clearance space is of maximum capacity to decrease the water flow velocity to prevent the water from washing against the core. This is achieved by increasing the outer diameter of the drill bit and cutters (Fig. 14). (2) Alternately, some holes can be drilled in the lower end of the outer wall to disperse the force of impact of the water. (3) A long inner wall is also useful to protect the ice cores.

4. Conclusion

A coring system using a PDM to convert the hydraulic pressure of water flow into rotation and torque, based on a HWD system, was designed in this study. The coring system mainly consisted of an anti-torque system and PDM, core barrel, and drill bit. A new self-adaptable leaf spring anti-torque device was used to adapt to the irregular boreholes created by the HWD system.

The required force-energy parameters of the PDM were estimated theoretically. A PDM with a lobe number of 3:4 was found to be suitable with a rotor and stator of diameters 56 mm and 38 mm, respectively. The pressure drop was determined to be not more than 0.33 MPa and the displacement per revolution was 0.66 L/r.

The test results showed that the use of relatively low-temperature water was more appropriate for the coring system. A double-walled core barrel was more suitable than a single-walled core barrel and ice cores with a maximum diameter of 84 mm were obtained. This showed that the PDM coring system worked adequately with a core barrel inner diameter of 89 mm, water flow rate of 96 L/min, and water temperature of 5 °C.

A PDM with the distinct technical parameters that were calculated will be processed and field testing of the coring system has been planned at the Amery Ice Shelf, East Antarctica in the future as a part of the Chinese Hot-water Drilling Project.

Acknowledgments

This study was conducted with the support of the National Natural Science Foundation of China (Project No. 41706214 and Project No. 41506216) and Program for Jilin University Science and Technology Innovative Research Team (Project No. 2017TD-24). The authors would like to thank the anonymous reviewers and scientific editor for their fruitful suggestions, useful comments, and editing.

References

Baldenko, D., Korotaev, Y., 2002. Positive displacement motors: 35 years on service of a petroleum industry. Neftyanoe Khoz. 11, 48–51.
Bentley, C.R., Koci, B.R., 2007. Drilling to the beds of the Greenland and Antarctic ice sheets: a review. Ann. Glaciol. 47 (1), 1–9.
Bentley, C.R., Koci, B.R., Augustin, L.J.-., Bolsey, R.J., Green, J.A., Kyne, J.D., Lebar, D. A., Mason, W.P., Shturmakov, A.J., Engelhardt, H.F., Harrison, W.D., Hecht, M.H., Zagorodnov, V., 2009. Ice Drilling and Coring. Drilling in Extreme Environments: Penetration and Sampling on Earth and Other Planets. Wiley-VCH Verlag GmbH & Co. KGaA, Weinheim, pp. 221–308.
Casey, K., Fudge, T., Neumann, T., Steig, E., Cavitte, M., Blankenship, D., 2014. The 1500 m South Pole ice core: recovering a 40 ka environmental record. Ann. Glaciol. 55 (68), 137–146.
Craven, M., Allison, I., Fricker, H.A., Warner, R., 2009. Properties of a marine ice layer under the Amery ice shelf, East Antarctica. J. Glaciol. 55 (192), 717–728.
Das, D.K., Koci, B.R., Kelley, J.J., 1992. Development of a thermal mechanical drill for sampling ice and rock from great depths. Tunn. Undergr. Space Technol. Inc. Trenchless 7 (4), 377–382.
Engelhardt, H., Humphrey, N., Kamb, B., Fahnestock, M., 1990. Physical conditions at the base of a fast moving antarctic ice stream. Science 248 (4951), 57–59.
Engelhardt, H., Kamb, B., Bolsey, R., 2000. A hot-water ice-coring drill. J. Glaciol. 46 (153), 341–345.
Fan, X., Talalay, P.G., Zheng, Z., Zhang, N., Cao, P., Yu, D., Hu, Z., Yang, C., 2016. Design of antitorque system of cable-suspended electromechanical drill for subglacial bedrock coring. J. Cent. South Univ. 47 (3), 946–952.
Han, C., Zhang, J., Liang, Z., 2014. Thermal failure of rubber bushing of a Positive Displacement Motor: a study based on thermo-mechanical coupling. Appl. Therm. Eng. 67 (1–2), 489–493.
Haynes, W.M., 2017. In: CRC Handbook of Chemistry and Physics: a Ready-Reference Book of Chemical and Physical Data, 98th (2017-2018). CRC Press, Boca Raton.
Jackson, M., Kamb, B., 1997. The marginal shear stress of Ice Stream B, West Antarctica. J. Glaciol. 43 (145), 415–426.
Koci, B., 1994. THE AMANDA Project: drilling precise, large-diameter holes using hot water. Mem. Natl. Inst. Polar Res. - Special Issue 49, 203–211.
Langway, C.C., 2008. The history of early polar ice cores. Cold Reg. Sci. Technol. 52 (2), 101–117.
Lowder, D.M., Halzen, F., Morse, R., Price, P.B., Barwick, S.W., Miller, T., Westphal, A., 1991. Observation of muons using the polar ice cap as a Cerenkov detector. Nature 353 (6342), 331–333.

Makinson, K., 1994. BAS hot water drilling on Ronne Ice Shelf, Antarctica. Mem. Natl. Inst. Polar Res. 49, 192–202. Special Issue.

Makinson, K., 2006. Future Hot Water Drilling on Rutford Ice Stream 2004/05. Forum for Research into Ice Shelf Processes (FRISP) Report No 14.

Makinson, K., Anker, P.G.D., 2014. The BAS ice-shelf hot-water drill: design, methods and tools. Ann. Glaciol. 55 (68), 44–52.

Makinson, K., Pearce, D., Hodgson, D.A., Bentley, M.J., Smith, A.M., Tranter, M., Rose, M., Ross, N., Mowlem, M., Parnell, J., Siegert, M.J., 2016. Clean subglacial access: prospects for future deep hot-water drilling. Philos. Trans. R. Soc. A Math. Phys. Eng. Sci. 374 (2059), 20140304.

Nguyen, T.C., Al-Safran, E., Nguyen, V., 2018. Theoretical modeling of positive displacement motors performance. J. Pet. Sci. Eng. 166, 188–197.

Nicholls, K.W., Corr, H.F.J., Makinson, K., Pudsey, C.J., 2012. Rock debris in an Antarctic ice shelf. Ann. Glaciol. 53 (60), 235–240.

Rignot, E., Jacobs, S., Mouginot, J., Scheuchl, B., 2013. Ice-shelf melting around Antarctica. Science 341 (6143), 266–270.

Robles, J., 2001. Another look to multilobe progressive cavity pump. In: SPE Progressing Cavity Pump Workshop, Puerto La Cruz.

Samuel, G.R., 1997. Mathematical Modeling and Design Analysis of the Power Section of a Positive Displacement Motor (PDM).

Schwander, J., Marending, S., Stocker, T.F., Fischer, H., 2014. RADIX: a minimal-resources rapid-access drilling system. Ann. Glaciol. 55 (68), 34–38.

Silvestri, A., AMANDA Collaboration, 2005. The AMANDA neutrino telescope. Int. J. Mod. Phys. A 20 (14), 3096–3098.

Su, Y., 2001. Research and Application of Positive Displacement Motor. Petroleum Industry Press, pp. 34–36.

Sugiyama, S., Sawagaki, T., Fukuda, T., Aoki, S., 2014. Active water exchange and life near the grounding line of an Antarctic outlet glacier. Earth Planet. Sci. Lett. 399, 52–60.

Talalay, P.G., 2003. Power consumption of deep ice electromechanical drills. Cold Reg. Sci. Technol. 37 (1), 69–79.

Talalay, P.G., Fan, X., Zhang, Z., Xue, J., Cao, P., Zhang, N., Wang, R., Yu, D., Yu, C., Zhang, Y., Zhang, Q., Su, K., Yang, D., Zhan, J., 2014. Anti-torque systems of electromechanical cable-suspended drills and test results. Ann. Glaciol. 55 (68), 207–218.

Talalay, P.G., Pyne, A.R., 2017. Geological drilling in McMurdo dry valleys and McMurdo sound, Antarctica: historical development. Cold Reg. Sci. Technol. 141, 131–162.

Vogel, S.W., Tulaczyk, S., Kamb, B., Engelhardt, H., Carsey, F.D., Behar, A.E., Lane, A.L., Joughin, I., 2005. Subglacial conditions during and after stoppage of an antarctic ice stream: is reactivation imminent? Geophys. Res. Lett. 32 (14), L14502.

Wang, R., Liu, A., Sun, Y., Cao, P., Fan, X., Talalay, P., 2018. Ice drill testing facility. Cold Reg. Sci. Technol. 145, 151–159.

White, F.M., 2011. Fluid Mechanics, seventh ed. McGraw-Hill, New York.